ISSN (Print) : 2320 – 3765
ISSN (Online): 2278 – 8875

International Journal of Advanced Research in Electrical, Electronics and Instrumentation Engineering

(An ISO 3297: 2007 Certified Organization)

Website: www.ijareeie.com

Vol. 6, Issue 6, June 2017

High-Gain Soft Switching Bidirectional Converter with Coupled Inductor

Sanoop B[1], Dr.K N Pavithran[2]

PG Student [Power System and Control], Dept. of EE, Govt. Engg College BartonHill,Trivandrum, Kerala, India[1]

Professor, Dept of EE, Govt. Engg College BartonHill, Trivandrum, Kerala, India[2]

ABSTRACT:In recent years the usage of renewable energy sources are increasing day by day. Solar being a reliable and inexhaustible source of energy is being widely utilized in areas like standalone solar photovoltaic systems, solar heating and cooling and electric vehicle applications. This paper proposes high gain bidirectional dc-dc converter using a coupled inductor for electric vehicle systems. By using a high gain converter the size of battery bank used at the input of the converter can be reduced resulting in substantial reduction in size, weight and cost of the system. The circuit operates in zero voltage switching condition and bidirectional operation is achieved with the help of three switches, a coupled inductor and an active clamp circuit. The analysis of both buck and boost modes of a 300w system is also presented in this paper.

KEYWORDS: Bidirectional dc-dc converter, coupled inductor, zero voltage switching (ZVS).

I.INTRODUCTION

Bi-directional DC-DC Converters are widely used in many applications such as hybrid vehicles, battery charging/discharging DC converters in UPS system. Usually in electric vehicle battery bank are the energy source which provides low voltage at the input of the bidirectional converter. The string of batteries connected in series has some disadvantages. A larger battery bank increases the size and cost of the system. Also if there is a mismatch in the batteries voltage or difference in the batteries temperature with in the string, it will cause charge imbalance in the battery bank [1]. Therefore this paper focuses on the analysis and design of a high efficiency bidirectional converter with high voltage conversion ratio. This will help in reducing the number of batteries in the input and hence the size and cost of the system.

II.LITERATURE SURVEY

Isolated bridge-type bidirectional converters are the most popular topology in high power applications. But more number of switches is to be used causing large value of switching losses. More than that voltage and current stresses in the switches is high. Conduction losses are high due to the presence of large number of switches. Thus the implementation will be complex.

In a non-isolated technology the bulky galvanic isolation transformer along with several switches are eliminated leading to reduction in switching losses and the cost. With incorporation of coupled inductor and zero voltage switching (ZVS), Non-isolated bidirectional converters has attracted special interest due to high conversion ratio, reduced switching losses, and simplicity in design [2]. These types of topologies are highly cost effective and acceptable due to high efficiency improvement, and considerable reduction in the weight and volume of the system.This paper proposes a new non-isolated bidirectional DC-DC converter with coupled inductor. The proposed converter has following advantages.

1. High Voltage Gain in both the buck and boost mode
2. Only three active switches are used to perform bidirectional operation.
3. Less number of passive components are used in the circuit
4. Zero voltage switching (ZVS), synchronous rectification, and voltage clamping circuit are used which reduces the switching and conduction losses.

The renewable energy sources, like the photovoltaic (PV) energy have been attracted a lot of attentions and are becoming an effective solution to overcome the environmental pollution and energy shortage problems. The

ISSN (Print) : 2320 – 3765
ISSN (Online): 2278 – 8875

International Journal of Advanced Research in Electrical, Electronics and Instrumentation Engineering

(An ISO 3297: 2007 Certified Organization)

Website: www.ijareeie.com

Vol. 6, Issue 6, June 2017

coordination control schemes among various converters have been proposed to harness maximum power from renewable power sources, to proper power transfer between ac and dc loads, and to maintain the stable operation of both ac and dc grids under variable supply and demand conditions. The advanced power electronics and control technologies used in this paper will make a future power grid much smarter.

III.CONVERTER OPERATION

The configuration of the proposed circuit is shown in the Fig. 1. The Low Voltage Side (LVS) of the bidirectional converter is connected with the battery bank and the high voltage side (HVS) is connected to the high voltage DC bus. Coupled inductor has been used with L_P as primary inductance and L_S as the secondary inductance tightly coupled on the same ferrite core. The polarities of the primary and secondary windings keep changing, depending on the switchesPWM. The inductor is custom based designed depending on the turn ratio and the voltages of LVS and HVS.

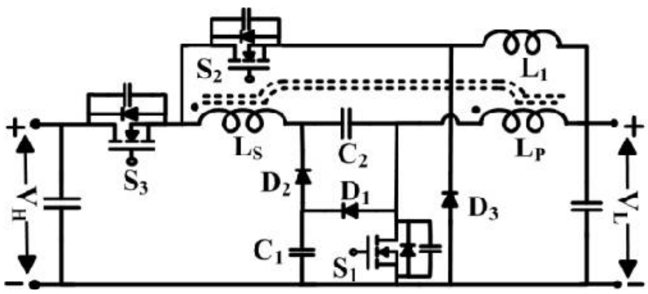

Fig.1 Proposed ZVS non-isolated bidirectional converter

Capacitor C_2 inserted in the main power across the primary and secondary windings of the transformer gives high voltage diversity and reduces the peak current stress allowing current in the primary continuous. Also the voltage stress of the capacitor C_2 will be minimum at this position. The circuit can operate both in the buck mode to recharge the battery and boost mode to provide the regulated high DC output voltage.

A. Buck Mode of Operation:

The characteristic waveforms of the converter during buck mode of operation are shown in Fig. 2. D_1 is the duty ratio of S_1 and S_2, where D_3 is the duty ratio of switch S_3. Both D_1 and D_3 are related to each other by a relationship D_1 (= 1− D_3). The coupled inductor can be modeled as an ideal transformer with the magnetizing inductor Lm andturns ratio

$N = N_2/N_1$, where N_1 and N_2 are the winding numbers in the primary and secondary side of the coupled inductor respectively.

Mode 1 ($t_0 \sim t_1$): The Switch S_3 remains ON while the switches S_1 & S_2 are OFF during mode 1. The current i_{LS} flows from High voltage side (HVS) to the Low Voltage Side (LVS) of the circuit through the capacitor C_2 and both the windings of the coupled inductor. Applying KVL we get (1).

$$V_H = V_{LS} + V_{C2} + V_{LP} + V_L \quad (1)$$

$$V_H = V_{LP}(1+N) + V_{C2} + V_L \quad (2)$$

The diode D_3 is also conducting with continuous inductor current i_{L1} into the low voltage side LVS of the circuit. Hence, V_L is the voltage across inductor L_1.

ISSN (Print) : 2320 – 3765
ISSN (Online): 2278 – 8875

International Journal of Advanced Research in Electrical, Electronics and Instrumentation Engineering

(An ISO 3297: 2007 Certified Organization)

Website: www.ijareeie.com

Vol. 6, Issue 6, June 2017

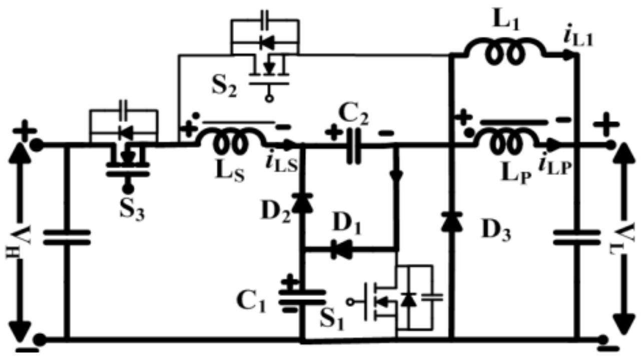

Mode 2 ($t_1 \sim t_2$): At the start, the switch S_3 turns OFF. Due to the storage energy in the leakage inductor, the polarities are reversed across the primary and secondary windings (L_S & L_P) of the coupled inductor. Switch S_3 is OFF in this mode, but the secondary current i_{LS} is still conducting, so the switch S_2 body diode turns ON in order to keep the current i_{LS} flowing. The diode D_3 keeps conducting in this mode. The switch S_1 body diode also turns ON because though the secondary current i_{LS} decreases, but the primary current i_{LP} remains the same.

Mode 3 (t2 ~ t3): Both the Switches S1 and S2 turn ON following zero voltage switching (ZVS) condition. The capacitor C2 starts discharging across LVS of the circuit through the switch S2 and inductor L1. Thus the secondary current is induced in reverse by discharging capacitor C2. Clamp capacitor C1 also discharge through the diode D2 by adding small current *i*3 into the secondary current flowing into the Low voltage side of the circuit. Using the voltage second balance, VC2 will be,

$$V_{C2} = V_{L1} + V_L + V_{LS} \quad (3)$$

The stored energy in the coupled inductor is released by primary current through the switch S_1 into LVS.
Using the voltage-second balance, the V_{L1} is given by,

$$D_1 V_{L1} = D_3 V_L \quad (4)$$

Primary winding voltage V_{LP} can be obtained as,

$$D_3 V_{LP} = D_1 V_L \quad (5)$$

Putting (4) and the values of V_{L1}, and V_{LP} in (2), the voltage gain during buck mode of operation is given by equation,

$$G_{buck} = V_L / V_H$$
$$= [D_3(1-D_3)] / [2N(1-D_3)^2+1] \quad (6)$$

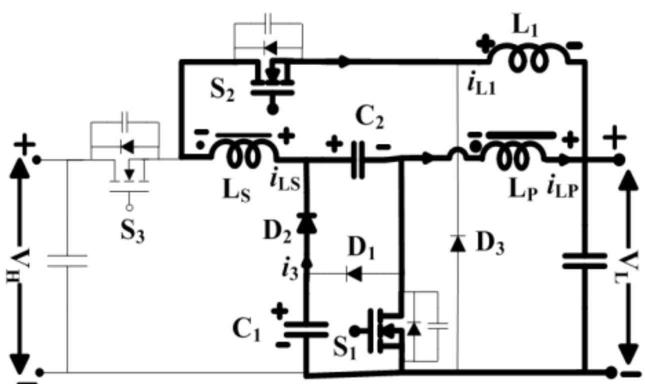

Mode 4 ($t_3 \sim t_4$): Both the switches S_1 and S_2 turn OFF at the start of this mode. The primary and secondary winding currents i_{LP} &i_{LS} will continue conduction due to the leakage inductance of the coupled inductor. The secondary current will charge the parasitic capacitance of the switches S_1 & S_2, and discharge the parasitic capacitance of the switch S_3. When the voltage across the switch S_2 equals to V_H, the body diode of the switch S_3 turns ON. The primary current i_{LP} starts decreasing unless it equals to the secondary current i_{LS}, then this mode finishes.

ISSN (Print) : 2320 – 3765
ISSN (Online): 2278 – 8875

International Journal of Advanced Research in Electrical, Electronics and Instrumentation Engineering

(An ISO 3297: 2007 Certified Organization)

Website: www.ijareeie.com

Vol. 6, Issue 6, June 2017

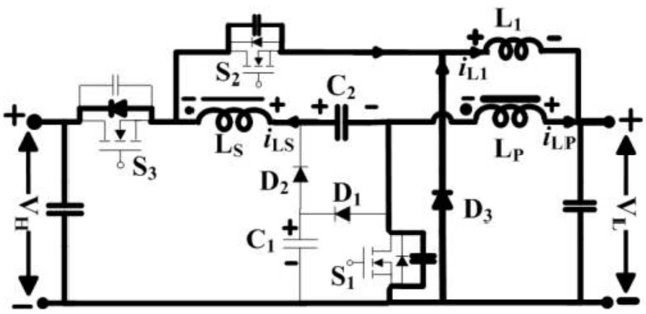

Mode 5 ($t_4 \sim t_5$): The switch S_3 turns ON under zero voltage switching (ZVS) condition. The capacitor C_1 is charges through the clamped Diode D_1. The primary and secondary current starts increasing. At the end of this mode, the circuit starts repeating mode 1of the next cycle.

B. Boost Mode of Operation

During boost mode, the proposed converter steps up the low-battery bank voltage to high dc-link voltage. Switch *S*2 remains OFF during the boost mode of operation. The operation of the circuit during boost mode is as below.

Mode 1 (t0 ~t1): Duringmode1, switch*S*1wasON, whereas switch *S*3 was OFF. Low-battery bank voltage is applied at the LVS of the circuit. Capacitor*C*2 remains charged before mode 1, and the magnetizing current *i*LM of the coupled inductor linearly increases, as shown in Fig. 3. Applying KVL, we get

$$VL = VLp = VLS/N. \quad (7)$$

The voltage across the primary winding can be derived using voltage-second balance, i.e.,

$$VLPD3 = VLD1.(8)$$

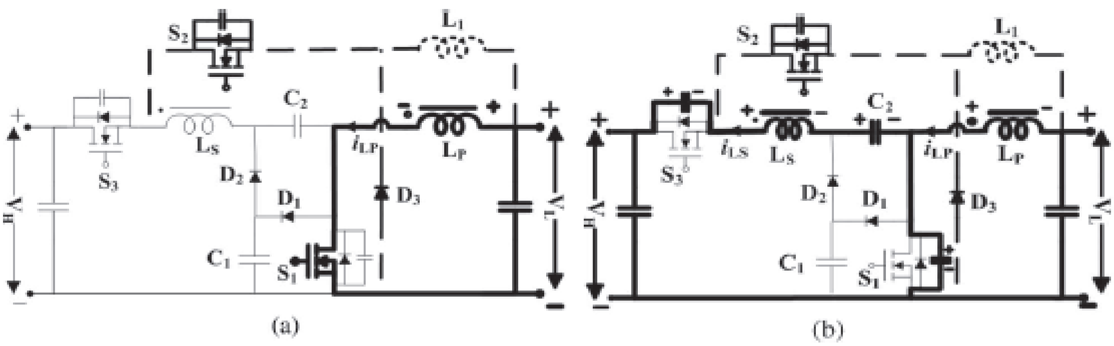

Mode 2 (t1 ~t2): Switch *S*1 turns OFF in mode 2. The primary current *i*LP charges the parasitic capacitance across switch S1, and the secondary current *i*LS discharges the parasitic capacitance across switch S3. When the voltage across switch S1 is equal to the capacitor voltage VC1, this mode finishes.**Mode 3 (t2 ~t3):**Since switch S1 is OFF, leakage inductance causes the primary current *i*LP to decrease while the secondary current *i*LS increases. As a result, the body diode of switch S3 turns ON. Capacitor C1 starts charging through diode D1 because the voltage across switch S1 gets higher than capacitor C1. This limits the voltage stress across switch S1. The voltage across the capacitor is given by

$$VC1 = VL + VLP. \quad (9)$$

Using (7)

$$VC1 = VL/D3. \quad (10)$$

ISSN (Print) : 2320 – 3765
ISSN (Online): 2278 – 8875

International Journal of Advanced Research in Electrical, Electronics and Instrumentation Engineering

(An ISO 3297: 2007 Certified Organization)

Website: www.ijareeie.com

Vol. 6, Issue 6, June 2017

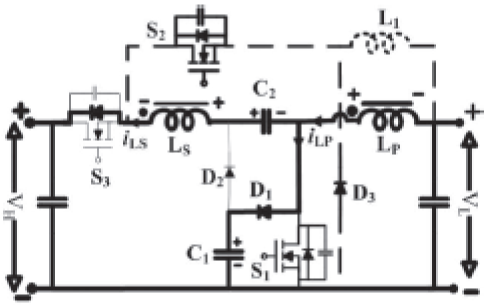

(c)

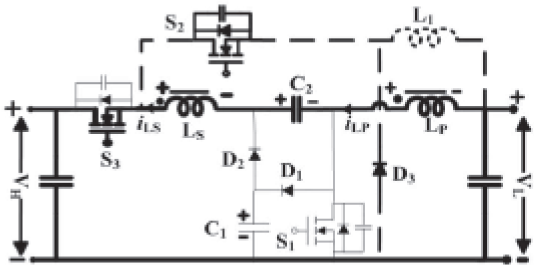

(d)

Mode 4 (t_3 ~t_4): Switch *S*3 turns ON under the condition Of ZVS. The primary and secondary windings of the coupled inductor and capacitor C2 are all now connected in series to transfer the energy to the HVS of the circuit. iLS starts increasing until it reaches iLP, then it follows iLP until the end of mode 4. Thus, the energy stored in the primary and secondary discharges across the HVS of the circuit. Both diodes D1 and D2 remain OFF during this mode, as shown in Fig. Using voltage-second balance, we get

$$VH = VL + VLS + VC2 + VLp \qquad (11)$$

$$VH = VL + VC2 + (N + 1)VLP . \qquad (12)$$

Mode 5 (t_4 ~t_5): During this mode, switch S3 turns OFF.The current iLS charges the parasitic capacitance of switch S3. Capacitor C1 starts discharging across capacitor C2, through diode D2, i.e.,

$$VC2 = VC1 = VL/D3. \qquad (13)$$

By putting (8) and (13) in (12), the voltage gain of the circuit is

$$VH = VL + VL/D3 + (N + 1)D1/D3VL \qquad (14)$$

$$\mathbf{Gboost} = \mathbf{VH/VL} = (\mathbf{2} + \mathbf{ND1})/(\mathbf{1} - \mathbf{D1}). \qquad (15)$$

The body diode of switch S1 turns ON because of the polarities of capacitor C2 and inductor LP.

Mode 6 (t_5 ~t_6): During Mode 6, switch S1 turns ON under the condition of ZVS. Since S1 is not deriving any current from the clamped circuit, the switching losses remain low due to ZVC, and the efficiency of the circuit increases. When both VC1 and VC2 get equal, the next switching cycle starts and repeats the operation in mode 1.

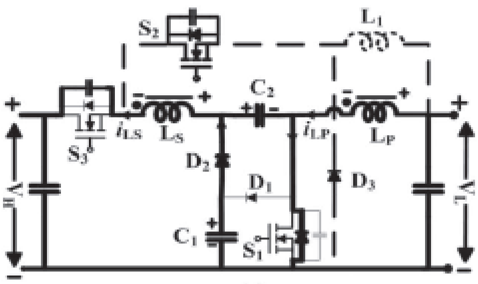

(e)

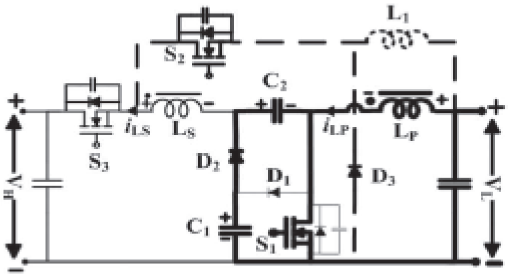

(f)

ISSN (Print) : 2320 – 3765
ISSN (Online): 2278 – 8875

International Journal of Advanced Research in Electrical, Electronics and Instrumentation Engineering

(An ISO 3297: 2007 Certified Organization)

Website: www.ijareeie.com

Vol. 6, Issue 6, June 2017

IV. DESIGN CONSIDERATIONS

Turns ratio of the coupled inductor must be selected to satisfy the voltage gain during both buck and boost mode of operation. Fig. 4 shows the voltage gain at both the buck and boost modes with respect to duty cycle D3 at different values of turns ratio N. Analysis of the graphs in fig.2 shows that the turns ratio N should be selected as N = 2.5.

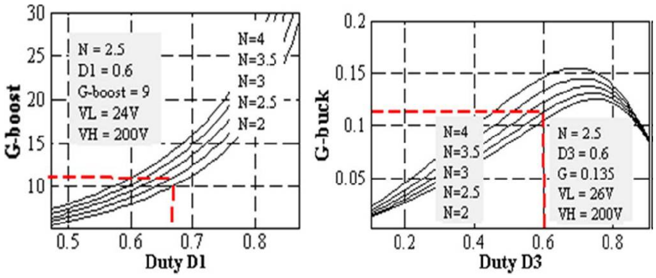

Fig.2 Gain duty ratio variation of converter

A. Coupled Inductor Design

To design a coupled inductor, analyze the circuit in either buck or boost mode of operation and calculate the magnetizing inductor Lm, and the number of turns N1 and N2 of the coupled inductor. The inductor needs to be high enough to minimize the ripple and associated losses. Consider boost mode of operation, the magnetizing current iLm when switch S1 turns ON is given by

$$iLm = (1/Lm)\, Vint + IL(0) \quad 0 \le t < DT \qquad (16)$$

where IL(0) is the initial current at t = 0. iLM, when switch S1 turns OFF and S3 ON, is given by

$$iLm = (1/Lm)\,[(Vo - 2Vin)/(2 + N)](t - D1T) + IL(D1T) \qquad (17)$$

Putting $t = D1T$ in (16) and $t = T$ in (17), we get

$$IL(D1T) - IL(0) = (1/Lm)Vin(D1T) \qquad (18)$$

$$IL(D1T) - IL(0) = -(1/Lm)\,[(2Vin - Vo)/(2 + N)](1 - D1T)T \qquad (19)$$

$$(Vo/Vin) = (2 + ND1)/(1 - D1) \qquad (20)$$

The ripple current in the inductor is given by

$$\Delta I = [(1/Lm)][\,(Vo(1 - D1)D1T)/(2 + ND1)] \qquad (21)$$

The average input current is given by

$$Iin = [\,ILm(max) + ILm(min)\,] / 2 \qquad (22)$$

The average output current

$$Io = Iin\,(1 - D1) = (Vo/R) \qquad (23)$$

$$I_{Lm(max)} = \left(\frac{2 + ND_1}{(1 - D_1)^2 R} + \frac{D_1 T}{2Lm}\right) \qquad (24)$$

ISSN (Print) : 2320 – 3765
ISSN (Online): 2278 – 8875

International Journal of Advanced Research in Electrical, Electronics and Instrumentation Engineering

(An ISO 3297: 2007 Certified Organization)

Website: www.ijareeie.com

Vol. 6, Issue 6, June 2017

Solving for critical magnetizing inductance value, which keeps the converter into continuous conduction mode, we set ILm (min) = 0

$$L_{m(\text{crit})} = \frac{D_1(1-D_1)^2 \text{RT}}{2(2+\text{ND}_1)} \qquad (25)$$

Thus number of turns can be obtained as

$$\frac{N_2}{N} = N_1 = \frac{L_m I_m}{B_{\max A_c}} 10^4 \qquad (26)$$

Bmax is the maximum flux density, and Ac is the core cross sectional area.

V. EXPERIMENTAL RESULTS

A 300W system is simulated in Mat-Lab for 24V input and 200V output. Both boost and buck operations are verified.ZVS condition of the main switches were also verified.

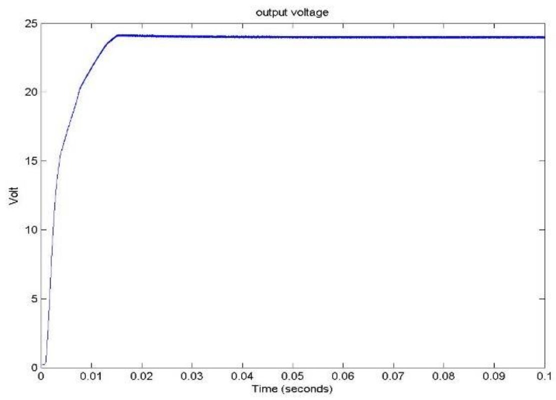

Fig. 3 Output voltage for buck mode of operation.

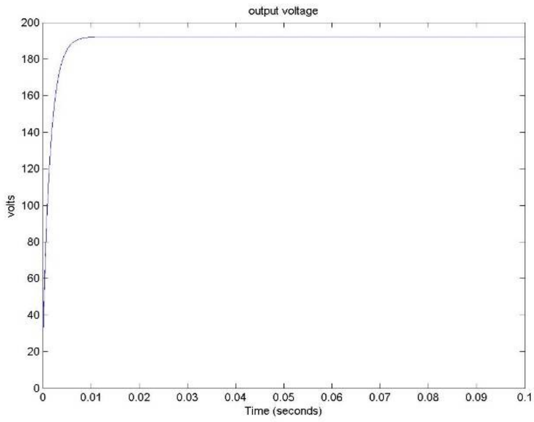

Fig. 4 Output voltage for boost mode of operation

Buck mode output of the converter is as shown in fig.3. as expected the output voltage is regulated at 24V.settling time is only 15 millisecond. The boost mode of the converter gives an output as shown in the fig.4. Output settles at 192V. Efficiency was obtained as 95% for buck and 93% for boost mode.

Fig.5 shows the zero voltage swiching of the main switch s2. It is observed that the current switching takes place during the zero voltage period. Two other switches also undergoes ZVS and was verified.

ISSN (Print) : 2320 – 3765
ISSN (Online): 2278 – 8875

International Journal of Advanced Research in Electrical, Electronics and Instrumentation Engineering

(An ISO 3297: 2007 Certified Organization)

Website: www.ijareeie.com

Vol. 6, Issue 6, June 2017

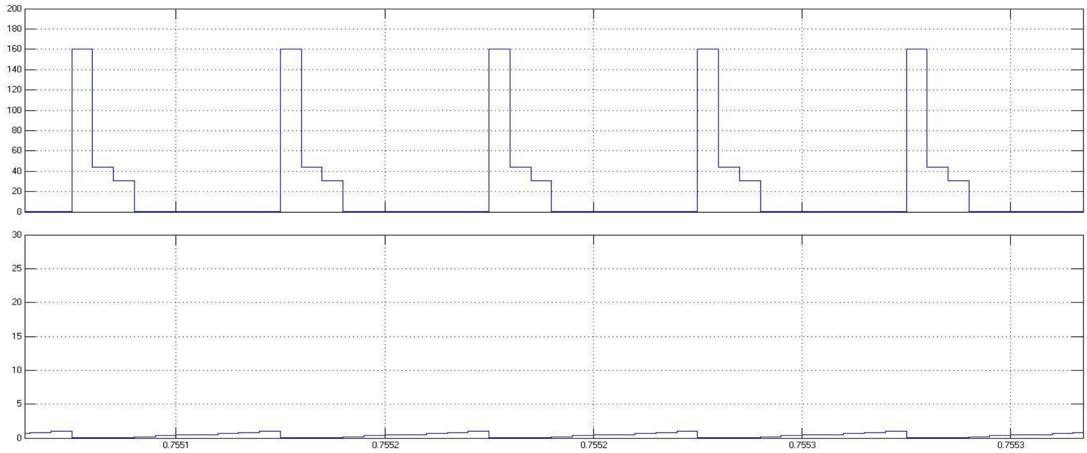

Fig.5 Zero voltage switching of main switch s2

VI. CONCLUSION

A non-isolated ZVS bidirectional dc–dc converter with a coupled inductor is discussed. The most promising features of the converter are a high voltage conversion ratio in both modes of operation, with less number of active switches, and low voltage and current stresses on the switches. The operation principle of each mode has been explained. Simulation results are verified including the ZVS operation of the switches.

REFERENCES

[1] Y.-P. Hsieh, J.-F. Chen, L.-S. Yang, C.-Y. Wu, and W.-S. Liu, "High-conversion-ratio bidirectional dc–dc converter with coupled inductor," IEEE Transactions on Industrial Electronics,pp. 210-222, Jan. 2014.

[2] P. Das, B. Laan, S. A. Mousavi, and G. Moschopoulos, "A non-isolated bidirectional ZVS-PWM active clamped DC–DC converter," IEEE Transactions on Power Electronics,vol. 24, pp. 553-558, Jan. 2009.

[3] C.-C. Lin, L.-S. Yang, and G. Wu, "Study of a non-isolated bidirectional DC–DC converter," IET Power Electronics, vol. 6, pp. 30- 37, Jan. 2013.

[4] H. Shiji, K. Harada, Y. Ishihara, T. Todaka, and G. ALZAMORA,“A zero-voltage-switching bidirectional converter for PV systems,” Instit.Electron., Inf. Commun. Eng. Trans. Commun., vol. 87, pp. 3554–3560,Oct. 2004.

[5] M. Kwon, S. Oh, and S. Choi, “High gain soft-switching bidirectional DC–DC converter for eco-friendly vehicles,” IEEE Trans. Power Electron., vol. 29, no. 4, pp. 1659–1666, Apr. 2014.

.